Proceedings World Geothermal Congress 2015
Melbourne, Australia, 19-25 April 2015

Multi-Fluid Sedimentary Geothermal Energy Systems for Dispatchable Renewable Electricity

Thomas A. Buscheck[1], Jeffrey M. Bielicki[2,3,] Mingjie Chen[1], Yunwei Sun[1], Yue Hao[1], Thomas A. Edmunds[1], Jimmy B. Randolph[4], and Martin O. Saar[4,5]

[1]Atmospheric, Earth, and Energy Division, Lawrence Livermore National Laboratory (LLNL), Livermore, CA USA

[2]Department of Civil and Geodetic Engineering, The Ohio State University (OSU), Columbus, OH USA

[3]John Glenn School of Public Affairs, The Ohio State University (OSU), Columbus, OH USA

[4]Department of Earth Sciences, University of Minnesota, Minneapolis, MN USA

[5]Geothermal Energy and Geofluids Group, Department of Earth Sciences, ETH-Zürich, Zürich, CH

buscheck1@llnl.gov

Keywords: Geothermal, horizontal wells, parasitic load, working fluid, bulk energy storage, dispatchable power, renewable electricity

ABSTRACT

Sedimentary geothermal resources typically have lower temperatures and energy densities than hydrothermal resources, but they often have higher permeability and larger areal extents. Consequently, spacing between injection and production wells is likely to be wider in sedimentary resources, which can result in more fluid pressure loss, increasing the parasitic cost of powering the working fluid recirculation system, compared to hydrothermal systems. For hydrostatic geothermal resources, extracting heat requires that brine be lifted up production wells, such as with submersible pumps, which can consume a large portion of the electricity generated by the power plant. CO_2 is being considered as an alternative working fluid (also termed a supplemental fluid) because its advantageous thermophysical properties reduce this parasitic cost, and because of the synergistic benefit of geologic CO_2 sequestration (GCS). We expand on this idea by: (1) adding the option for multiple supplemental fluids (N_2 as well as CO_2) and injecting these fluids to create overpressured reservoir conditions, (2) utilizing up to three working fluids: brine, CO_2, and N_2 for heat extraction, (3) using a well pattern designed to store supplemental fluid and pressure, and (4) time-shifting the parasitic load associated with fluid recirculation to provide ancillary services (frequency regulation , load following, and spinning reserve) and bulk energy storage (BES).

Our approach uses concentric rings of horizontal wells to create a hydraulic divide to store supplemental fluid and pressure, much like a hydroelectric dam. While, as with any geothermal system, electricity production can be run as a base-load power source, production wells can alternatively be controlled like a spillway to supply power when demand is greatest. For conventional geothermal power, the parasitic power load for fluid recirculation is synchronous with gross power output. In contrast, our approach time-shifts much of this parasitic load, which is dominated by the power required to pressurize and inject brine. Thus, most of the parasitic load can be scheduled during minimum power demand or when, due to its inherent variability, there is a surplus of renewable energy on the grid. Energy storage is almost 100 percent efficient because it is achieved by time-shifting the parasitic load. Consequently, net power can nearly equal gross power during peak demand so that geothermal energy can be used as a form of high-efficiency BES at large scales. A further benefit of our approach is that production rates (per well) can exceed the capacity of submersible pumps and thereby take advantage of the productivity of horizontal wells and better leverage well costs—which often constitute a major portion of capital costs. Our vision is an efficient, dispatchable, renewable electricity system approach that facilitates deep market penetration of all renewable energy sources: wind, solar, and geothermal, while utilizing and permanently storing CO_2 in a commercially viable manner.

1. INTRODUCTION

Previous studies have investigated the performance of sedimentary geothermal energy production systems that use CO_2 as the heat extraction fluid (Randolph and Saar, 2011a, 2011b; Adams et al., 2014a; 2014b; Garapati et al., 2014) and multiple heat extraction fluids, CO_2, N_2, and brine (Buscheck et al., 2013c; 2014). Sedimentary formations are an under-explored play concept because they are typically associated with a conductive thermal regime, requiring greater depths to reach economic temperatures than hydrothermal upflows. On the other hand, sedimentary reservoirs offer the advantages of higher permeability (and transmissivity), extending over much larger areas (> 100 km^2) than typical upflows (< 3 km^2), and have lower, predictable drilling risk. These make an attractive target for geothermal development; however, larger well spacings may be needed for financial viability. To enable working fluid recirculation, such large well spacings require greater fluid overpressure (ΔP), defined to be fluid pressure in excess of ambient pressure, which can result in a greater parasitic load to drive fluid recirculation than in hydrothermal power systems. In this paper we examine how this parasitic load can be time-shifted to provide dispatchable renewable electricity and bulk energy storage (BES).

2. BACKGROUND

2.1 Geothermal Reservoir Management for Dispatchable Renewable Electricity

Geothermal reservoir management can compensate for imbalances between load and available generation on the grid. There are two fundamental ways in which geothermal resources can provide this service:

1. The *gross* power output from a geothermal power plant can be adjusted to match the variable supply from other grid resources with the actual demand by scheduling the timing and magnitude of energy withdrawal from the reservoir. This 'supply-response matching' approach may be applied to all types of geothermal power systems.

2. A portion of the parasitic load associated with power generation can be time-shifted to adjust the *net* power output. This 'time-shifting' approach depends on reservoir conditions and how heat is recovered from the reservoir; it can be particularly useful for overpressured reservoirs that do not require submersible pumps for heat recovery. The multi-fluid geothermal energy system approach, designed to create an overpressured reservoir, can stabilize electricity grids and provide BES by using cyclic-injection/pressure-augmentation, rather than steady-injection/pressure-augmentation to drive fluid recirculation.

The first approach does not use the full capacity of the geothermal power plant (and associated capital investment), and thus increases the levelized cost of electricity (LCOE). If variable heat withdrawal involves complete suspension of that withdrawal, it may also result in operational issues associated with exacerbated duty cycles from heating and cooling components of the power system. However, if variable heat withdrawal involves only the reduction of that withdrawal, rather than complete suspension, it will limit temperature fluctuations of the power system components. Further, variable heat withdrawal can delay the thermal decline of the reservoir, relative to the decline that would result from continuous withdrawal at full plant capacity. This delay would likely extend the useful lifetime of the geothermal power system and time-shift revenue to a later date, but this may decrease the net present value of the project, and thus negatively impact the financial viability of the system. However, if variable heat withdrawal is conducted on a diurnal basis, it will allow for increased power output during periods of high electricity demand, which can improve financial viability of the system.

The second approach (parasitic-load time-shifting) uses the full capacity (and the associated capital investment) of most of the components of the power plant, including the turbines and the injection and production wells. As a consequence, this approach will likely decrease the LCOE. The primary components that must be oversized, relative to the power plant capacity, are those involved with reinjecting the working fluids into the reservoir. Because this approach generates revenues that are typically associated with geothermal power sales, in addition to those associated with providing ancillary services (frequency regulation at sub-second time intervals, load following at five-minute intervals, and spinning reserve) and BES, it can further decrease the LCOE. Since the parasitic load can be scheduled to use the lowest-price electricity, the variable cost of electricity can be reduced. This approach allows the power turbines to spin continuously, and thus the plant can respond faster to grid imbalances. When most of the parasitic load is shifted to periods of low electricity demand, more power can be delivered to the grid when demand is high, because net power is nearly equal to gross power, which will increase revenues.

The second approach takes advantage of the fact that much of the parasitic load in geothermal power systems is associated with the power required to recirculate the working fluids for heat extraction, which is typically brine. For vapor-dominated reservoirs or liquid-dominated artesian reservoirs—which are naturally overpressured above hydrostatic pressure—most of the parasitic load is associated with reinjecting condensate or brine, or with transporting *make-up* water from a separate source and injecting it. For liquid-dominated hydrostatic reservoirs, most of the parasitic load is associated with lifting brine up the production wells. Submersible pumps, which typically provide this lift, can consume a large fraction of the electricity generated by the power plant. Because this parasitic load cannot be time-shifted, it is useful to find alternative means of driving fluid recirculation, as provided by the multi-fluid geothermal energy system approach (Buscheck et al., 2013c; 2014; Buscheck, 2014a; 2014b). For hydrostatic reservoirs, the parasitic load of brine reinjection is relatively small and time-shifting this load may not be useful. Because the power requirements for reinjecting brine into overpressured reservoirs can be relatively large, time-shifting this parasitic load can be a useful means of providing ancillary services (Edmunds et al., 2014), as well as providing large-scale BES over days to weeks or longer.

2.2 Multi-Fluid Geothermal Energy System Approach

The multi-fluid geothermal energy system approach injects supplemental fluids (in addition to native brine) to create overpressured reservoir conditions and to provide multiple working fluids for pressure augmentation, energy storage, and energy withdrawal (Buscheck, 2014a; 2014b). Building upon the CO_2-Plume Geothermal (CPG) concept (Saar et al., 2010; Randolph and Saar, 2011a; 2011b, 2011c), this approach injects a combination of CO_2 that is captured from the exhaust streams of fossil-energy systems and N_2 that is separated from air (Figure 1). Fluid-recirculation efficiency and per well fluid production rates are increased by the additional supplemental fluid and the advantageous thermophysical properties of those fluids, notably, their high mobilities (i.e., low kinematic viscosities) and high thermal coefficients of thermal expansion. Pressure augmentation is improved by the thermosiphon effect that results from injecting cold/dense CO_2 and N_2 (Adams et al., 2014). These fluids are geothermally heated to reservoir temperature, greatly expand, and thus increase the artesian flow of brine and supplemental fluid at the production wells.

The multi-fluid geothermal energy approach uses a well pattern consisting of a minimum of four concentric rings of horizontal producers and injectors (Figure 1) that creates a hydraulic divide designed to store pressure and supplemental fluid, segregate the supplemental fluid and brine production zones, and generate large artesian flow rates to better leverage the productivity of horizontal wells. Because fluid production is driven by stored pressure, it is possible to increase production when power demand is high or when there is a deficit of other renewable energy on the grid. It may also be advantageous to decrease production when demand is low or when there is a surplus of other renewable energy on the grid, which would serve to further store pressure and energy for use when demand exceeds supply. Supplemental-fluid injection enhances fluid production rates in several ways. The thermosiphon effect can result in large supplemental-fluid production rates. Supplemental-fluid injection also displaces brine to where it is produced at the inner production ring (Figure 1), creating "make-up" brine. Some of this make-up brine may be used to cool the power plant and reduce its water intensity, which can be particularly useful in water-constrained regions. The rest of the make-up brine can be reinjected into the third ring of horizontal wells to increase gross power output. Thus, the obvious benefit of CO_2 and N_2 injection is that it generates excess brine for reinjection through displacement. However, there is an additional benefit of this injection process, which is altering the pressure distribution within the reservoir. Recent studies (Buscheck et al., 2013d;

2014) found that a relatively small amount of N_2 or CO_2 can create a large "topographic high" in pressure (Figure 2b), allowing overpressured brine to be injected in the third ring of wells "uphill" from the "downhill" outer ring of brine producers (Figure 1).

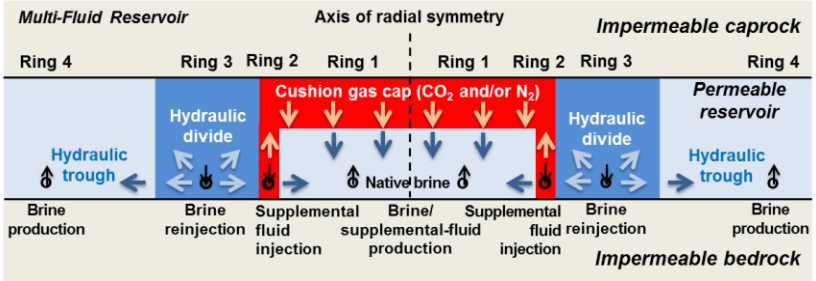

Figure 1: Multi-ring, horizontal-well configuration used in the multi-fluid geothermal energy system approach (Buscheck, 2014a; 2014b). For this study, all wells are located at the bottom of the permeable reservoir formation. Due to buoyancy, supplemental fluid migrates to the top of the permeable reservoir to form a "cushion gas" cap that increases the pressure-storage capacity of the system. Note that this is not to scale. See Table 2 for well spacings.

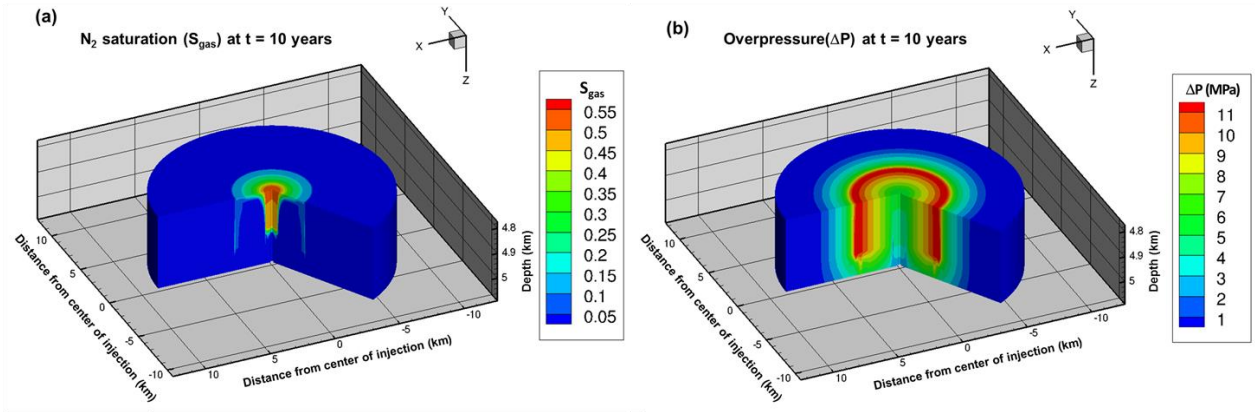

Figure 2: Distributions of (a) N_2 saturation and (b) overpressure (ΔP) at 10 years (Buscheck et al., 2013d). The region of high ΔP corresponds to the hydraulic divide in Figure 1.

A key feature of our approach is the option of time-shifting the parasitic load associated with fluid recirculation to achieve BES. As discussed later, the parasitic load is dominated by the power required to pressurize and inject brine. By comparison, the power required to compress and inject CO_2 is negligible, while the power required for N_2 injection is about 10 to 25 percent that of brine. Because N_2 can be readily separated from air and produced brine can be temporarily stored in surface holding ponds, N_2 and brine injection can be scheduled during periods of low power demand or when there is a surplus of renewable energy on the grid. Time-shifting when the parasitic load is imposed can reduce the cost of powering fluid recirculation in addition to providing BES. Our system can be pressurized (recharged) when supply exceeds demand; the system can be depressurized (discharged) when demand exceeds supply. Thus, our approach shares some of the attributes of pumped storage hydro (PSH) and its subsurface equivalent, underground pumped hydro storage (UPHS). Because of their compressibility, supercritical CO_2 and N_2 function as cushion gases to provide enormous storage capacity—similar to compressed air energy storage (CAES). However, unlike air used in CAES, N_2 is non-corrosive and will not react with the reservoir formation. Because the ability to store energy increases with the ability to store pressure and because pressure-storage capacity increases with the volume of cushion gas, BES capacity increases with stored CO_2 and N_2 mass.

Our approach has potential operational advantages over conventional geothermal systems. Large centralized pumps located on the surface may be more efficient than submersible pumps. Moreover, surface-based pumps would not be exposed to the harsh conditions in production wells and not require the frequent maintenance that could disrupt production. Our approach would be particularly valuable in hydrostatic reservoirs where temperatures are too hot (> 200°C) for submersible pumps to survive. It could also result in flow rates greater than the capacity of submersible pumps (80 to 120 kg/sec), which would increase leveraging of well costs.

3. MODELING APPROACH

We conduct reservoir analyses with the Nonisothermal Unsaturated Flow and Transport (NUFT) numerical simulator, which simulates multi-phase heat and mass flow and reactive transport in porous media (Nitao, 1998; Hao et al., 2012). NUFT has been used extensively in reservoir studies of geologic CO_2 sequestration (GCS) and of multi-fluid geothermal systems (Buscheck et al., 2012; 2013b; 2013c; 2014). The values of pore and water compressibility are 4.5×10^{-10} Pa^{-1} and 3.5×10^{-10} Pa^{-1}, respectively. Water density is determined by the ASME (2006) steam tables. The two-phase flow of supercritical CO_2 and water is simulated with the density and compressibility of supercritical CO_2 determined by the correlation of Span and Wagner (1996) and CO_2 dynamic

viscosity being given by the correlation of Fenghour et al. (1997). The two-phase flow of supercritical N_2 and water is simulated with the density and compressibility for N_2 determined by the correlation of Span et al. (2000) and the dynamic viscosity being taken from Lemmon and Jacobsen (2004).

To gain first-order insights, a generic system (Figure 1) is modeled over the course of 30 years, which is equivalent to the multi-fluid system considered in our related study of vertically stacked reservoirs (Saar et al., 2015). The system consists of a 125-m-thick reservoir with a permeability of 1×10^{-13} m^2, bounded by low-permeability seal units (caprock and bedrock) each with a permeability of 1×10^{-18} m^2. Hydrologic properties (Table 1) are similar to previous GCS and multi-fluid geothermal studies (Zhou et al., 2008; Buscheck et al., 2013a; 2013b; 2013c; 2014; Elliot et al., 2013). Because conditions are assumed to be laterally homogeneous, we use a radially-symmetric (RZ) model. A geothermal gradient of 37.5°C/km and reservoir bottom depths of 3, 4, and 5 km are considered. The initial temperature at the bottom of the reservoir is 127.0, 164.5, and 202.0°C for the three depths, respectively, assuming an average surface temperature of 14.5°C. The RZ model is thus a simplified representation of an actual system, but likely representative of rings of arc-shaped horizontal wells, which, in actual geothermal reservoir system implementations may be horizontal partial-circles that intercept inclined reservoir-caprock or vertically offset fault interfaces. Using an RZ model allows for fine mesh refinement, particularly around the injectors and producers to better model pressure gradients close to the wells. The dimensions of the four-ring well configuration are listed in Table 2.

Table 1: Hydrologic and thermal properties used in this study.

Property	Reservoir	Seal units (caprock and bedrock)
Permeability (m^2)	1.0×10^{-13}	1.0×10^{-18}
Thermal conductivity (W/m°C)	2.0	2.0
Porosity	0.12	0.12
van Genuchten (1980) *m*	0.46	0.46
van Genuchten α (1/Pa)	5.1×10^{-5}	5.1×10^{-5}
Residual supercritical fluid saturation	0.05	0.05
Residual brine saturation	0.30	0.30

Table 2: Four-ring well-field case considered in this study.

Well-field footprint area (km^2)	Well-ring radius (km)				Inner swept area (km^2)	Outer swept area (km^2)
	Ring 1 brine/CO_2 producers	Ring 2 CO_2 injectors	Ring 3 brine injectors	Ring 4 brine producers		
64	0.5	2.0	2.5	4.5	11.8	44.0

For this study, NUFT is used to model pure supercritical CO_2 or N_2 injection. We use the reservoir model results to determine brine-based, Organic Rankine Cycle (ORC) binary-power generation, using the GETEM code (DOE, 2012). Geothermal energy is extracted from produced N2 or CO2 at the surface using a direct-cycle power system, in which the produced N2 or CO2 is itself sent through a turbine rather than a binary-cycle power system. For N2 or CO2 as a working fluid, direct-power systems offer much greater energy conversion efficiency than binary systems (Adams et al., 2014) because the supercritical fluids generate a substantial pressure difference between the hot production wellhead and the cold injection wellhead, while simultaneously losing considerable temperature during their rise in production wells. The latter effect—Joule-Thomson cooling—causes low binary-system efficiency compared to brine-based systems operating at similar reservoir temperatures (Adams et al., 2014). We assume that produced brine has been separated from the produced N2 or CO2 prior to sending the N2 or CO2 through the turbine to generate electricity. Because the energy penalty for fluid separation is minor, we have neglected it from our power-generation analyses.

Past CPG and multi-fluid geothermal studies have considered a wide range of CO_2 and N_2 injection rates (Randolph and Saar, 2011c; Buscheck et al., 2013b; 2013c; 2014; Adams et al, 2014; Garapati et al., 2014). Several of these studies have considered CO_2 injection rates that would be associated with CO_2 captured from large fossil-energy power plants (Randolph and Saar, 2011c; Buscheck et al., 2013a; 2013b; 2014). Recently, it was found that such large CO_2 and N_2 injection rates can lead to large overpressure ΔP in the reservoir that will drive up the parasitic load for pressurizing and injecting brine, resulting in less efficient power generation (Buscheck et al., 2014). Thus, for this study, we consider a narrower range of initial supplemental-fluid (N_2 or CO_2) injection rates, ranging from 15 to 120 kg/sec. For all cases, the maximum N_2 or CO_2 injection rate is specified to be no greater than twice the initial rate. For most cases, the N_2 or CO_2 injection rate gradually increases to the maximum rate, which allows produced N_2 or CO_2 to be recirculated and to extract more heat from the reservoir. The initial-maximum N_2/CO_2 injection-rate scenarios are denoted "15-30", "30-60", "60-120", and "120-240", respectively. All produced N_2 or CO_2 is reinjected into the second ring of horizontal wells and all produced brine is reinjected into the third ring of horizontal wells (Figure 1). Power is generated from produced CO_2 or N_2 in a direct system and from brine in an indirect (i.e., binary ORC) system. It is assumed that the exit temperature of the brine from the binary-cycle power plant is cooled so that is enters the reservoir at a temperature of 65°C. After N_2 and CO_2 have passed through the direct-cycle turbine, N_2 and CO_2 are assumed to have cooled to such a temperature at the injection well head that after compression in the injection well, the temperature of the N_2 and CO_2 entering the reservoir at depth is 25°C. The CO_2 that is delivered from the fossil-energy system source is also assumed to enter the reservoir at 25°C.

4. RESULTS AND DISCUSSION

The results of this study are presented in two parts. In Section 4.1, we assume synchronous parasitic loading and constant heat withdrawal, which is typical of most geothermal power systems, when analyzing the dependence of power generation to supplemental-fluid (N_2 or CO_2) injection rate and geothermal resource depth/temperature. In Section 4.2, we examine how dispatchable power and diurnal BES can be achieved by time-shifting the parasitic load associated with brine pressurization and injection and by varying heat withdrawal rate. The influence of supplemental-fluid injection rate and geothermal resource depth/temperature on dispatchable power and BES is also addressed.

4.1 Power Generation with Synchronous Parasitic Loading and Constant Heat Withdrawal

Figure 3 summarizes temperature, overpressure, and power over the 30-year production period. Tables 3–6 summarize power performance at 10 years, which is close to when peak power occurs (Figure 4). We begin with the most apparent dependencies. Net power and gross power (Figures 3a and b) increase strongly with resource depth/temperature (Figure 3c). While gross power increases monotonically with initial supplemental injection rate, net power does not, for reasons discussed below. For initial supplemental-fluid injection rates > 30 kg/sec, temperature decline increases with supplemental-fluid injection rate (Figure 3c). Temperature decline is also greater for N_2 injection because the lower density of N_2 displaces more brine than does CO_2.

Net power increases more quickly with time for higher supplemental-fluid injection rates (Figure 4). Net power also increases more quickly for N_2 injection than for CO_2 injection because the smaller density of N_2, compared to CO_2, displaces more brine than does an equivalent mass of CO_2. The increased rate of fluid displacement causes heat to be swept more quickly from the formation, which increases the rate of thermal decline (Figure 3d). Accordingly, net power declines more quickly at higher supplemental-fluid injection rates, with lower supplemental-fluid injection rates sustaining net power for longer periods, which will extend the economic lifetime of the reservoir system.

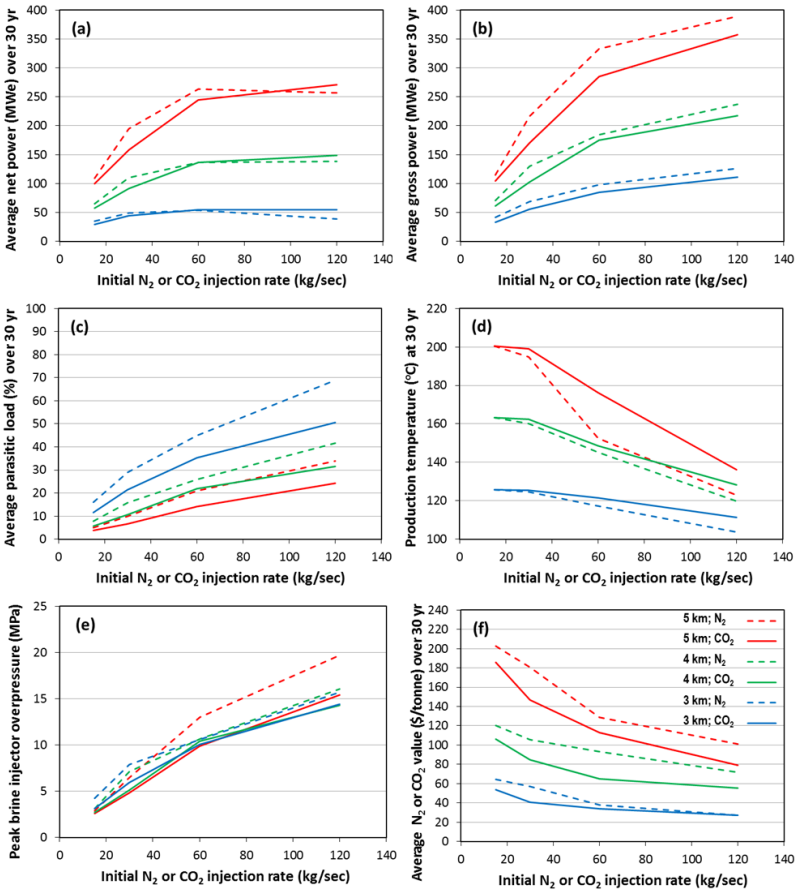

Figure 3: Temperature, overpressure, and power are summarized for reservoir depths of 3, 4, and 5 km and for initial N_2 and CO_2 injection rates ranging from 15 to 120 kg/sec. The average unit N_2 and CO_2 values are based on total power sales at $100/MWh over a period of 30 yr.

As indicated in recent studies of multi-fluid geothermal power systems (Buscheck et al., 2014), reservoir pressure management is a key consideration for engineering efficient heat extraction, and power generation. Gross power increases with supplemental-fluid injection rate (Figure 3b); however, for initial supplemental-fluid injection rates > 60 kg/sec, net power does not increase much for CO_2 injection, and actually decreases slightly for N_2 injection (Figure 3a). The primary reason for this trend is the dependence of parasitic load (Figure 3c) on overpressure (Figure 3e), which increases with supplemental-fluid injection rate. The other reason for this trend is that the rate of thermal decline increases with supplemental-fluid injection rate (Figure 3d). While it would seem to be advantageous to minimize the parasitic load by reducing the supplemental-fluid injection rate, this also results in a reduction in net power output for supplemental-fluid injection rates < 60 kg/sec, with decreased leveraging of the well-field infrastructure cost. Therefore, the need to manage the parasitic load needs to be balanced against the need to sufficiently leverage the well-field infrastructure cost.

In addition to efficient net power generation, another financial consideration for reservoir operations is the efficient utilization of the supplemental fluid. The cost of CO_2 capture from fossil-energy systems may result in the cost of delivered CO_2 being greater than $40/tonne. Because the per unit cost of separating N_2 from air is much less than the cost of CO_2 capture, the cost of delivered N_2 will likely be much less than that of CO_2; however, it is still an important financial consideration for efficient reservoir operations. Figure 3f plots the unit value of N_2 and CO_2, assuming electricity power sales of $100/MWh.

Table 3: Power performance at 10 years is summarized for cases with an initial N_2 or CO_2 injection rate of 120 kg/sec and a maximum N_2 or CO_2 injection rate of 240 kg/sec.

Depth (km)	Supplemental fluid	Gross power (MWe)	N_2 or CO_2 parasitic load		Brine parasitic load		Net power (MWe)		
			MWe	% of gross	MWe	% of gross	After total parasitic load	After N_2/CO_2 parasitic load	Net power ratio*
5	N_2	558.4	18.7	3.4	158.3	28.3	381.5	539.7	1.41
	CO_2	495.5	2.1	0.4	115.8	23.8	377.6	493.4	1.31
4	N_2	285.7	14.6	5.1	110.3	38.6	175.4	271.2	1.55
	CO_2	273.4	2.0	0.7	86.6	31.7	184.9	271.5	1.49
3	N_2	142.1	10.3	7.0	85.2	58.1	51.1	136.3	2.67
	CO_2	121.8	1.4	1.1	61.8	50.2	62.8	124.6	1.99

Note: *Net power ratio is the net power after N_2/CO_2 parasitic load divided by the net power after total parasitic load. It is a measure of how much the time-shifting of the brine parasitic load can increase net power when it is demanded by the electricity grid.

Table 4: Power performance at 10 years is summarized for cases with an initial N_2 or CO_2 injection rate of 60 kg/sec and a maximum N_2 or CO_2 injection rate of 120 kg/sec.

Depth (km)	Supplemental fluid	Gross power (MWe)	N_2 or CO_2 parasitic load		Brine parasitic load		Net power (MWe)		
			MWe	% of gross	MWe	% of gross	After total parasitic load	After N_2/CO_2 parasitic load	Net power ratio*
5	N_2	420.2	4.3	1.0	75.6	18.0	340.3	415.9	1.22
	CO_2	331.8	0.5	0.1	42.5	12.8	288.9	331.3	1.15
4	N_2	231.8	6.8	2.0	59.4	17.9	169.3	228.7	1.35
	CO_2	190.7	0.4	0.2	36.5	19.2	153.8	190.3	1.24
3	N_2	115.7	4.5	3.9	50.4	43.6	60.7	111.2	1.83
	CO_2	99.5	0.3	0.3	36.7	31.8	62.6	99.3	1.59

Note: *Net power ratio is the net power after N_2/CO_2 parasitic load divided by the net power after total parasitic load. It is a measure of how much the time-shifting of the brine parasitic load can increase net power when it is demanded by the electricity grid.

Table 5: Power performance at 10 years is summarized for cases with an initial N_2 or CO_2 injection rate of 30 kg/sec and a maximum N_2 or CO_2 injection rate of 60 kg/sec.

Depth (km)	Supplemental fluid	Gross power (MWe)	N_2 or CO_2 parasitic load		Brine parasitic load		Net power (MWe)		
			MWe	% of gross	MWe	% of gross	After total parasitic load	After N_2/CO_2 parasitic load	Net power ratio*
5	N_2	249.5	2.00	1.3	22.0	14.7	225.5	247.5	1.10
	CO_2	185.2	0.2	0.1	11.3	6.1	173.7	185.0	1.07
4	N_2	141.2	1.5	1.1	20.0	13.1	121.1	139.7	1.15
	CO_2	108.2	0.1	0.1	10.4	9.5	97.8	108.1	1.10
3	N_2	77.4	1.0	1.3	21.9	27.1	55.5	76.4	1.38
	CO_2	58.3	0.1	0.2	11.3	19.2	47.0	58.2	1.24

Note: *Net power ratio is the net power after N_2/CO_2 parasitic load divided by the net power after total parasitic load. It is a measure of how much the time-shifting of the brine parasitic load can increase net power when it is demanded by the electricity grid.

Table 6: Power performance at 10 years is summarized for cases with an initial N_2 or CO_2 injection rate of 15 kg/sec and a maximum N_2 or CO_2 injection rate of 30 kg/sec.

Depth (km)	Supplemental fluid	Gross power (MWe)	N_2 or CO_2 parasitic load		Brine parasitic load		Net power (MWe)		
			MWe	% of gross	MWe	% of gross	After total parasitic load	After N_2/CO_2 parasitic load	Net power ratio*
5	N_2	111.7	1.0	0.9	4.9	4.4	105.9	110.7	1.05
	CO_2	108.0	0.1	0.1	4.3	4.0	103.6	107.9	1.04
4	N_2	73.1	0.7	1.0	5.5	7.6	66.8	73.4	1.08
	CO_2	67.3	0.1	0.1	4.4	6.5	62.8	67.2	1.07
3	N_2	46.0	0.6	1.3	8.2	17.9	37.3	45.4	1.22
	CO_2	36.7	0.04	0.1	4.8	13.1	31.9	36.7	1.15

Note: *Net power ratio is the net power after N_2/CO_2 parasitic load divided by the net power after total parasitic load. It is a measure of how much the time-shifting of the brine parasitic load can increase net power when it is demanded by the electricity grid.

4.2 Dispatchable Power Generation with Time-Shifted Parasitic Loading and Variable Heat Withdrawal

The previous results assume synchronous parasitic loads and constant heat withdrawal rate. In this section we investigate how time-shifting the parasitic load of pressurizing and injecting brine can provide dispatchable power and diurnal BES. We also consider how varying heat withdrawal rates can add to dispatchable power and diurnal BES. Because of the wide spacing between injection and production wells, the parasitic load associated with fluid recirculation ranges from being relatively large (Tables 3 and 4), compared to typical hydrothermal systems, to being relatively small (Tables 5 and 6), if the supplemental-fluid rate is small enough. The parasitic load associated with CO_2 compression and injection is too small to be useful for BES, while the parasitic load of N_2 compression and injection is large enough to be useful, particularly for seasonal BES (Buscheck et al., 2014). The parasitic load of pressurizing and injecting brine comprises about 75 to 99 percent of the total parasitic load for fluid recirculation for N_2 and CO_2 injection (Tables 3–6). Thus, time-shifting the brine injection parasitic load can be particularly useful for BES.

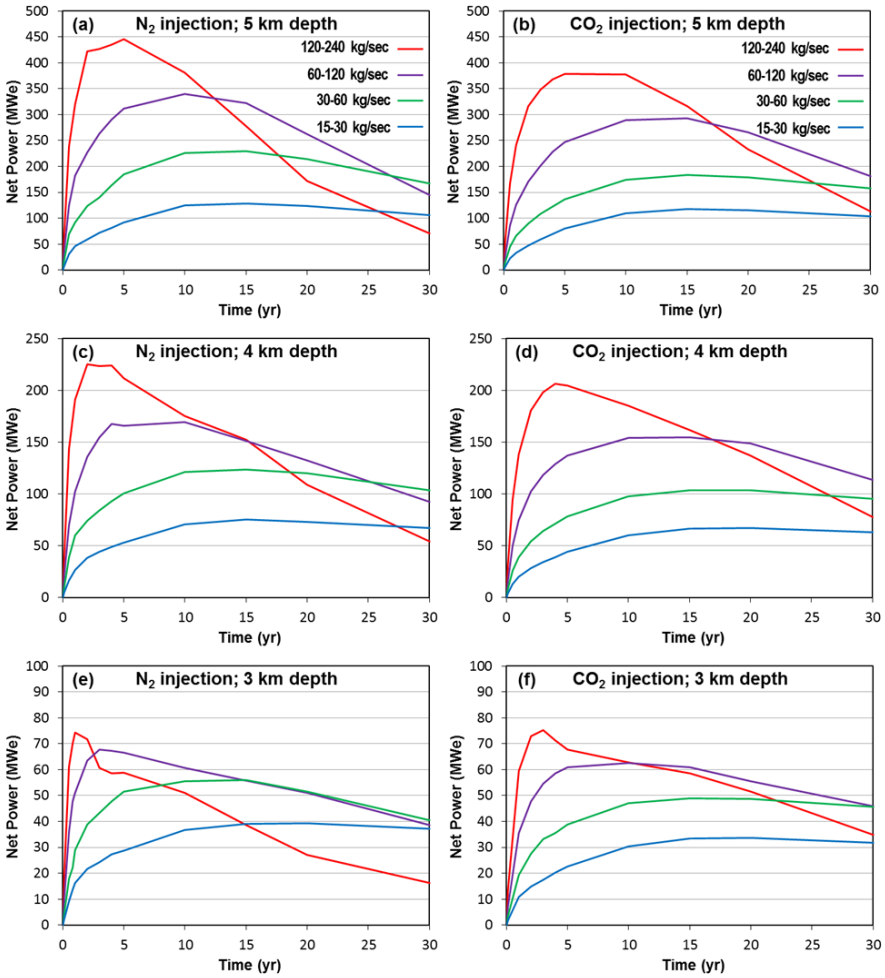

Figure 4: Net power time series are plotted for N_2 and CO_2 injection. Cases include reservoir depths of 3, 4, and 5 km and initial-maximum N_2 or CO_2 injection rates of 15-30, 30-60, 60-120, and 120-240 kg/sec. Note the different vertical scales for net power.

For BES, we categorize geothermal energy system operations into two time periods.

1. **Recharge period:** when the brine (and possibly N_2) parasitic load is entirely imposed. During this period, heat withdrawal rate can also be reduced in order to achieve negative net power generation, which corresponds to taking (storing) energy from the electricity grid.
2. **Discharge period:** when only the minor (N_2 or CO_2) parasitic loads are imposed. During this period, net power is nearly equal to gross power and energy that was stored during the recharge period is returned to the electricity grid. The net power ratio (see Tables 3–6) is net power during the discharge period, divided by constant (or average) net power that would occur with synchronous parasitic loading and constant heat withdrawal.

The net power ratio increases with the brine parasitic load (Table 3–6), which is the parasitic load that is being time-shifted in the BES cases plotted in Figure 5. For this paper, net power ratio is a measure of how much the time-shifting of the brine parasitic load can increase net power when it is demanded by the electricity grid, compared to the conventional case of synchronous parasitic loading. Figure 5 illustrates examples of diurnal BES where the time-shifted brine parasitic load ranges from 23.8 to 58.1 percent of gross power output, resulting in a net power ratio ranging from 1.31 to 2.67. The diurnal BES cycle consists of a 6-hour recharge period and an 18-hour discharge period. Two BES cases are shown: (1) BES case A, which time-shifts brine parasitic loading for a

6/18-hour recharge/discharge cycle and (2) BES case B, which is the same as case A, and reduces heat withdrawal rate by 50 percent during recharge. In all but one case (Figure 5b); BES case A yields a negative net power, corresponding to taking (storing) energy from the grid. When variable heat withdrawal is added, all six cases yield negative net power during recharge. For the 3-km deep reservoir, the net power ratio is 2.67 and 1.99 for N_2 and CO_2 injection, respectively. When operated with synchronous parasitic loading and constant heat withdrawal rate, the 3-km deep N_2 injection case generates a net power of 51.1 MWe, whereas applying a 6/18-hour recharge/discharge cycle allows it to generate +136.3 and -204.4 MWe during discharge and recharge, respectively. When heat withdrawal rate is reduced by 50 percent during the recharge period, it generates +155.8 and -272.5 MWe, during discharge and recharge, respectively. Clearly, the added benefit of multi-fluid BES can enhance the financial viability of what would otherwise be considered a marginal geothermal resource, while simultaneously promoting implementation of other, intermittently available, renewable energy sources, such as wind and solar, by providing a large-scale energy storage solution.

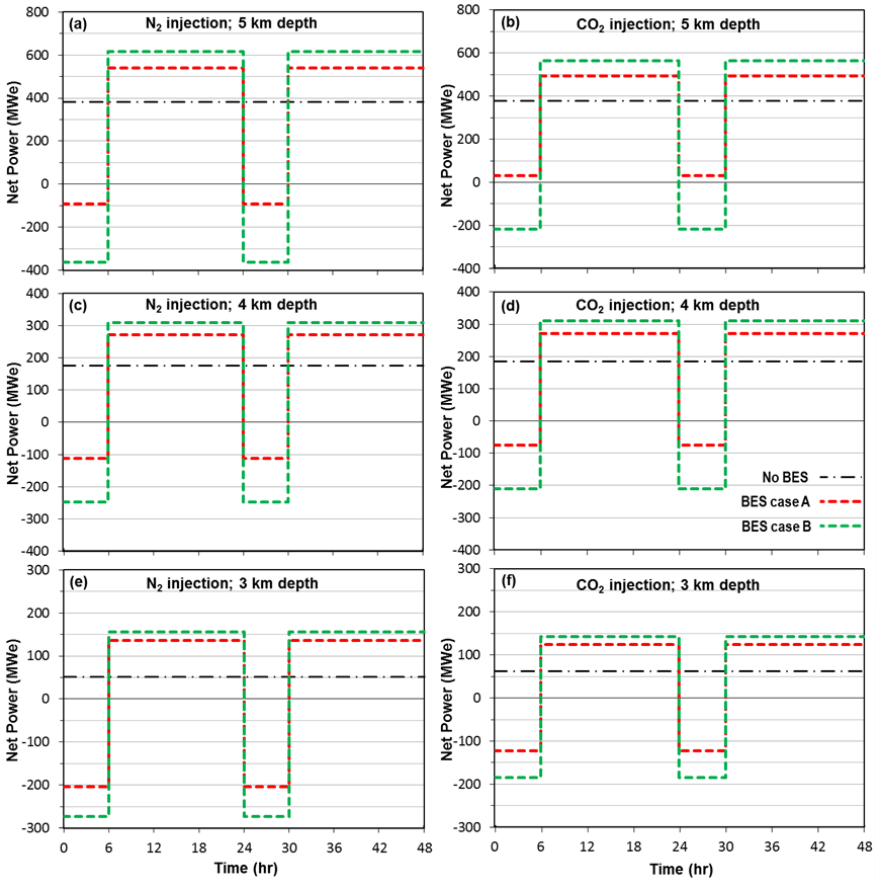

Figure 5: Net power time series are plotted over a 48-hour period that occurs 10 years into production for an initial N2 or CO2 injection rate of 120 kg/sec and a maximum N2 or CO2 injection rate of 240 kg/sec and reservoir depths of 3, 4, and 5 km. Time series are plotted for three cases: (1) no BES, with synchronous parasitic loading and constant heat withdrawal rate, (2) BES case A, which time-shifts the brine parasitic load to a 6-hour recharge period every 24 hours, and (3) BES case B, which reduces heat withdrawal rate by 50 percent and time-shifts the brine parasitic load during a 6-hour recharge period every 24 hours.

To first order, the magnitude of parasitic load is insensitive to geothermal resource depth/temperature (Table 3–6). Thus, for deeper/higher-temperature geothermal resources, because gross power is greater, the parasitic load (as a percentage of gross power) is considerably less than it is with shallower/lower-temperature resources. Moreover, the cases considered in this study assume just one value of permeability (1×10^{-13} m^2) for the geothermal reservoir. For higher values of permeability, ΔP and parasitic load would be less, while for lower values of permeability, ΔP and parasitic load would be greater than those of this study.

To provide a broader perspective on how diurnal BES operations might benefit a range of geothermal resources, including efficient, high-temperature resources, we consider a generic geothermal power plant with a net power output of 100 MW when operated with synchronous parasitic loading and constant heat withdrawal rate. Brine parasitic loads of 10 to 70 percent and recharge/discharge periods of 8/16, 6/18, 4/20, 3/21, and 2/22 hours are considered. Table 7 shows the benefit of time-shifting the brine parasitic load, while Table 8 adds the benefit of reducing heat withdrawal rate by 50 percent during the recharge period. Note that while Tables 7 and 8 are illustrated as pertaining specifically to diurnal BES, they can also pertain to longer-term BES, where, rather than listing the time period, the core variable of interest is the ratio between recharge and discharge durations. Because time-shifting the brine parasitic load requires temporary storage of brine in a lined retention pond at the ground surface, a limiting consideration is the required storage capacity of the retention pond. A second consideration would be that, compared to diurnal brine storage, longer-term surface storage of produced brine would allow for more cooling of the stored brine prior to reinjection, which could lead to increased thermal decline, as the reinjected brine reaches the brine production wells.

For efficient, high-temperature resources (e.g., 15 percent parasitic load), if the recharge duration is relatively long (e.g., eight hours per day), net power is positive during recharge, and power is not taken (stored) from the electrical grid (Table 7). However, if the parasitic load can be imposed during a sufficiently compressed recharge window (e.g., two hours per day), a 100 MW power plant with a 15 percent parasitic load could deliver 117.6 MW to the grid during the 22-hour discharge period and store -94.1 MW from the grid during the 2-hour recharge window (Table 7). If for that same case, heat withdrawal from the reservoir and corresponding gross power output from the power plant were reduced by 50 percent during the 2-hour recharge window, that plant could deliver 122.8 MW during discharge and store -159.6 MW during recharge (Table 8).

For a less efficient geothermal resource (e.g., 30 percent parasitic load), if heat withdrawal is held constant and an 8/16 hour recharge/discharge cycle is used, net power is equal to +142.9 and +14.3 MWe during discharge and recharge, respectively (Table 7). If for this same case, heat withdrawal is reduced by 50 percent during recharge and the recharge window is reduced by a factor of two (to a 4/20 hour cycle), net power during discharge increases to +155.8 MWe and is reduced to -202.6 MWe during recharge (Table 8). If for that case, the recharge window were further reduced to a 2/22 hour cycle, that power plant could store -462.1 MW during recharge (Table 8). Thus, increasing the capacity of the brine pumping/injection system can substantially increase BES capacity. A limiting consideration is the injectivity of the brine injection wells; however, the use of horizontal wells will facilitate higher injectivity than vertical wells. Because of the existence of a large N_2 or CO_2 *cushion* gas cap (Figure 1), reservoir pressure fluctuations during diurnal BES operations will be very small, as was demonstrated in a recent reservoir study of cyclic N_2 injection (Buscheck et al., 2014). An advantage of having the capacity to compress the recharge window is that it can take advantage of periods of over-generation when the price of electricity is small or possibly negative. Energy prices in the California ISO market spiked to -$100/MWh six times during 2013 (Edmunds et al., 2014). It is worth noting that in all of these diurnal BES examples, the power turbines are always spinning, which will limit temperature fluctuations of the power system components.

Table 7: Net power is listed for the discharge period and recharge period when the listed parasitic load is time-shifted to entirely occur during the recharge period. Gross power output is held constant during the entire 24-hour diurnal BES cycle. When the geothermal power plant is operated with no BES, the net power output is 100 MWe.

Recharge/discharge periods	Parasitic load	Net power (MWe)							
		10%	15%	20%	30%	40%	50%	60%	70%
8/16 hr	discharge	111.1	117.6	125.0	142.9	166.7	200.0	250.0	333.3
	recharge	77.8	64.7	50.0	14.3	-33.3	-100.0	-200.0	-366.7
6/18 hr	discharge	111.1	117.6	125.0	142.9	166.7	200.0	250.0	333.3
	recharge	66.7	47.1	25.0	-28.6	-100.0	-200.0	-350.0	-600.0
4/20 hr	discharge	111.1	117.6	125.0	142.9	166.7	200.0	250.0	333.3
	recharge	44.4	11.8	-25.0	-114.3	-233.3	-400.0	-650.0	-1066.7
3/21 hr	discharge	111.1	117.6	125.0	142.9	166.7	200.0	250.0	333.3
	recharge	22.2	-23.5	-75.0	-200.0	-366.7	-600.0	-950.0	-1533.3
2/22 hr	discharge	111.1	117.6	125.0	142.9	166.7	200.0	250.0	333.3
	recharge	-22.2	-94.1	-175.0	-371.4	-633.3	-1000.0	-1550.0	-2466.7

Note: The listed parasitic load is that which is being time-shifted (e.g., brine parasitic load or N_2/CO_2 plus brine parasitic load).

Table 8: Net power is listed for the discharge period and recharge period when the listed parasitic load is time-shifted to entirely occur during the recharge period. Gross power output is reduced by 50 percent during the recharge period. When the geothermal power plant is operated with no BES, the net power output is 100 MWe.

Recharge/discharge periods	Parasitic load	Net power (MWe)							
		10%	15%	20%	30%	40%	50%	60%	70%
8/16 hr	discharge	133.3	141.2	150.0	171.4	200.0	240.0	300.0	400.0
	recharge	26.7	17.6	-15.0	-68.6	-140.0	-240.0	-390.0	-640.0
6/18 hr	discharge	127.0	134.5	142.9	163.3	190.5	228.6	285.7	381.0
	recharge	12.7	-3.4	-42.9	-114.3	-209.5	-342.9	-543.9	-876.2
4/20 hr	discharge	121.2	128.3	136.4	155.8	181.8	218.2	272.7	363.6
	recharge	-12.1	-51.3	-95.5	-202.6	-345.5	-545.5	-845.5	-1345.5
3/21 hr	discharge	118.5	125.5	133.3	152.4	177.8	213.3	266.7	355.6
	recharge	-35.6	-87.8	-146.7	-289.5	-444.4	-746.7	-1146.7	-1858.6
2/22 hr	discharge	115.9	122.8	130.4	149.1	173.9	208.7	260.9	347.8
	recharge	-81.2	-159.6	-247.8	-462.1	-747.8	-1147.8	-1747.8	-2747.8

Note: The listed parasitic load is that which is being time-shifted (e.g., brine parasitic load or N_2/CO_2 plus brine parasitic load).

By exploiting diurnal variation in bulk energy prices, BES can provide additional revenues to geothermal plant operators. Historical price patterns observed in California in the year 2013 are shown in Figure 6 (OASIS 2014). In the figure, wholesale prices are color coded in accordance with the $/MWh scale shown on the right. Energy prices vary significantly during the course of a day−from

$20/MWh during the early morning hours to over $100/MWh during summer peak loads. During other times of the year prices vary from $20/MWh to $60/MWh. These prices can by overlain on the net power production patterns shown in Figure 5 to show the daily revenues for different well configurations and operating policies shown in that figure. Results are shown in Table 9.

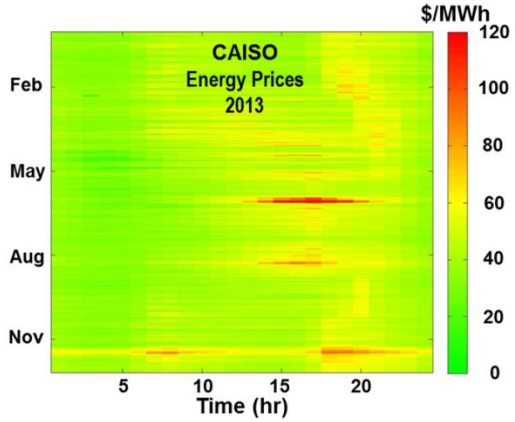

Figure 6: Wholesale energy prices in California are plotted for the year 2013 (Edmunds et al., 2014). Prices in $/MWh are color coded in accordance with the scale on the right. Periods of high prices, exceeding $100/MWh, occur during peak summer loads and during a period in early December. Prices drop to approximately $20/MWh during the early morning hours. Prices average approximately $60/MWh during other periods.

Table 9: Daily revenues ($) are listed for six reservoir cases (Figure 5) with and without BES. Prices are assumed to be $20/MWh for six off peak hours, $100/MWh for six on peak hours and $60/MWh during other periods.

Reservoir depth	Supplemental fluid (figure #)	No BES Synchronous parasitic loading and constant heat withdrawal rate ($)	BES Case A Time-shift brine parasitic load for a 6/18 hour cycle		BES Case B Time-shift brine parasitic load and 50% reduction of heat withdrawal rate for a 6/18 hour cycle	
			($)	Ratio*	($)	Ratio*
5 km	N_2 (5a)	548,640	701,640	1.29	770,880	1.41
	CO_2 (5b)	542,880	654,360	1.21	718,560	1.32
4 km	N_2 (5c)	252,000	344,280	1.37	378,240	1.50
	CO_2 (5d)	266,400	348,720	1.31	384,000	1.44
3 km	N_2 (5e)	73,440	155,040	2.11	173,160	2.36
	CO_2 (5f)	90,720	148,920	1.64	165,360	1.82

Note: *Ratio is equal to revenues for the BES case divided by the revenues for the case with no BES.

These three energy prices and the dispatch patterns for different resource depths/temperatures and operating policies shown in Figure 5 can be used to develop a rough estimate of daily revenues from diurnal BES. Assume the minimum energy price of $20/MWh is paid to support parasitic loads during the first 6 hours of the day, the maximum energy price of $100/MWh is received for six hours of the day, and $60/MWh is received for the remaining 12 hours of the day. Under these assumptions, daily revenues are shown in Table 9 for each of the 18 cases shown in Figure 5.

The data in the table indicate that daily revenues can be significantly enhanced relative to constant power generation by using diurnal BES. For the first case, N_2 injection into the deep (5-km depth) reservoir, daily revenues are increased by 41 percent if the brine parasitic load is shifted to a 6-hour window and gross production is reduced by 50 percent during that window, which corresponds to off peak hours. BES daily revenue gains range from 21 percent to greater than 100 percent for the other cases. BES more than doubles the daily revenues for N_2 injection in the shallow (3-km depth) reservoir. BES gains for CO_2 injection are more modest, but still approach a factor of two for the shallow reservoir depth.

5. FUTURE WORK

This study provides first-order insights into the potential of multi-fluid geothermal energy production and storage systems for a relatively simple generic, layered reservoir system with a single homogeneous, isotropic value of reservoir permeability and a single value of reservoir thickness. Future work needs to address a broad range of reservoir conditions (permeability and thickness) that may be encountered in real geologic settings. In addition, the influence of permeability heterogeneity and anisotropy, as well as laterally compartmentalization, needs to be considered, constrained by data from specific geologic settings.

Based on this study and past work, the use of CO_2 and N_2 injection each have their respective advantages; thus, staged supplemental-fluid injection (using both CO_2 and N_2) would be a useful strategy to examine in future work. Such work should investigate first-stage N_2 injection, followed by continuous CO_2 injection, together with cyclic/modulated N_2 injection, which is designed to modulate the parasitic load and thereby provide ancillary services, such as load following at five-minute intervals. With regards to well-field operations, an important goal to be examined would be for the inner ring of producers to first produce N_2 prior

to the arrival of CO_2, which would help assure that CO_2 could be produced without encountering conditions that would cause it to flash in the wellbore. All production wells will flow native brine prior to the arrival and production of the injected supplemental fluid. The concern is that during the transition period between brine and supplemental-fluid production, the pressure gradient in the wellbore may be large enough to cause CO_2 to flash prior to its reaching the wellhead, which could result in the Joule-Thomson cooling effect causing freezing inside the wellbore. If N_2 is the supplemental fluid flowing up the well during this transition period, the Joule-Thomson effect will not result in freezing, even if flashing occurs. Therefore, it would be beneficial if N_2 were the only supplemental-fluid present in the wellbore during the transition period. Subsequently, when CO_2 arrives at a well that is flowing N_2, the pressure gradient in the well will not be large enough to cause CO_2 to flash and possibly cause freezing.

Future work should also address economics of power generation, ancillary services (frequency regulation at sub-second time intervals, load following at five-minute intervals, and spinning reserve), and BES, with the cost of importing captured CO_2 versus the cost of separating N_2 from air being a consideration. Such work should consider actual electrical-grid supply/demand histories, examining how both brine and N_2 parasitic injection loads can be modulated in response to grid imbalances for a range of timescales. This work should include assessments of capital and operating costs in determining the overall economic viability of the multi-fluid geothermal approach to providing dispatchable power and BES.

6. CONCLUSIONS

We investigated the use of supplemental fluids (N_2 or CO_2) as pressure-augmentation and working fluids for geothermal energy production from sedimentary reservoirs, using a unique subsurface well design composed of four concentric rings of wells. These rings allow us to strategically create a hydraulic divide that constrains the migration of injected fluids and stores energy. The inner swept area is important because it is where the supplemental fluid eventually recirculates and where fluid displacement generates excess brine to be reinjected in the third well ring. The outer swept area, where only brine recirculates, is important because it is where the majority of heat extraction occurs from the geothermal reservoir. Because of the lower per area geothermal heat density associated with sedimentary reservoirs, larger spacings than in typical hydrothermal geothermal energy systems between the injection and production wells are necessary. Such well spacings will result in larger values of fluid overpressure and parasitic load associated with driving fluid recirculation than in typical hydrothermal systems. However, there is an important *return on investment* with regards to the larger parasitic loads, which is that it is likely to drive higher per well fluid production rates than those typically achievable with the use of submersible pumps. Because pressure is stored, the parasitic load associated with pressurizing and injecting brine, with comprises the majority of the parasitic load required to drive fluid recirculation, can be time-shifted to achieve diurnal and possibly longer-term bulk energy storage and to increase net power output when it is demanded by the electricity grid. In this way, multi-fluid geothermal energy systems appear to represent a promising approach to providing dispatchable renewable electricity and large-scale bulk energy storage, which are crucial to enabling the increased penetration of temporally variable renewable energy sources, such as wind and solar, to electricity grids.

ACKNOWLEDGMENTS

This study was funded by the U.S. Department of Energy (DOE) Geothermal Technologies Office (GTO) under grant number DE-FOA-0000336, a U.S. National Science Foundation (NSF) Sustainable Energy Pathways (SEP) grant, CHE-1230691. This work was performed under the auspices of the USDOE by Lawrence Livermore National Laboratory (LLNL) under DOE contract DE-AC52-07NA27344. We would also like to thank the Initiative for Renewable Energy and the Environment (IREE), a signature program of the Institute on the Environment (IonE) at the University of Minnesota (UMN), for initial seed funding. M.O.S. also thanks the ETH-Zürich (ETHZ) for its endowment support of the Geothermal Energy and Geofluids Group as well as the George and Orpha Gibson Endowment for its support of the Hydrogeology and Geofluids Group in the Department of Earth Sciences at UMN. Any opinions, findings, conclusions, or recommendations in this material are those of the authors and do not necessarily reflect the views of the DOE, NSF, IREE, IonE, UMN, ETHZ, or LLNL.

DISCLAIMER

Drs. Randolph and Saar have a significant financial interest, and Dr. Saar has a business interest, in Heat Mining Company LLC, a company that may commercially benefit from the results of this research. The University of Minnesota has the right to receive royalty income under the terms of a license agreement with Heat Mining Company LLC. These relationships have been reviewed and managed by the University of Minnesota in accordance with its conflict of interest policies.

REFERENCES

Adams, B., Kuehn, T.H., Bielicki, J.M., Randolph, J.B., and Saar, M.O.: On the importance of the thermosiphon effect in CO2-Plume Geothermal (CPG) systems, Energy, 69, (2014), 409-418.

ASME: ASME Steam Tables Compact Edition, ASME, Three Park Avenue, New York, NY, USA, (2006).

Brown, D.W.: A hot dry rock geothermal energy concept using supercritical CO2 instead of water, Proceedings of the 25th Workshop on Geothermal Reservoir Engineering, Stanford University, (2000), 233-238.

Buscheck, T.A., Sun, Y., Chen, M., Hao, Y., Wolery, T.J., Bourcier, W.L., Court, B., Celia, M.A., Friedmann, S.J., and Aines, R.D.: Active CO2 reservoir management for carbon storage: Analysis of operational strategies to relive pressure buildup and improve injectivity, International Journal of Greenhouse Gas Control, 6, (2012), 230-245.

Buscheck, T.A., Elliot, T.R., Celia, M.A., Chen, M., Sun, Y., Hao, Y., Lu, C., Wolery, T.J., and Aines, R.D.: Integrated geothermal-CO2 reservoir systems: Reducing carbon intensity through sustainable energy production and secure CO2 storage, Energy Procedia 37, (2013a), 6587-6594.

Buscheck, T.A., Chen, M., Lu, C. Sun, Y., Hao, Y., Celia, M.A., Elliot, T.R., Choi, H., and Bielicki, J.M.: Analysis of operational strategies for utilizing CO2 for geothermal energy production, Proceedings of the 38th Workshop on Geothermal Reservoir Engineering, Stanford University, Palo Alto, CA, (2013b).

Buscheck, T.A., Chen, M., Hao, Y., Bielicki, J.M., Randolph, J.B., Sun, Y., and Choi, H.: Multi-fluid geothermal energy production and storage in stratigraphic reservoirs, Proceedings for the Geothermal Resources Council 37th Annual Meeting, Las Vegas, NV, (2013c).

Buscheck, T.A., Bielicki, J.M., Randolph, J.B., Chen, M., Hao, Y., and Sun, Y.: Multi-fluid geothermal energy systems: Utilizing CO2 for dispatchable renewable power generation and grid stabilization, 2013 American Physical Union Fall Meeting, San Francisco, CA, (2013d).

Buscheck, T.A., Bielicki, J.M., Randolph, J.B., Chen, M., Hao, Y., Edmunds, T.A., Adams, B., and Sun, Y.: Multi-fluid geothermal energy systems in stratigraphic reservoirs: Using brine, N2, and CO2 for dispatchable renewable power generation and bulk energy storage, Proceedings of the 39th Workshop on Geothermal Reservoir Engineering, Stanford University, Palo Alto, CA, (2014).

Buscheck, T.A.: Systems and methods for multi-fluid geothermal energy systems, US Patent Application No. 14/167,375, filed January 29, 2014, published August 28, 2014, Application Publication No. 2014-0238672A1, (2014a).

Buscheck, T.A.: Multi-fluid renewable geo-energy systems and methods, US Patent Application No. 14/210,070, filed June 20, 2014, (2014b).

DOE: GETEM–Geothermal electricity technology evaluation model, August 2012 Beta, USDOE Geothermal Technologies Program, (2012).

Edmunds, T.A., Sotorrio, P., Bielicki, J.M., and Buscheck, T.A.: Geothermal power for integration of intermittent generation, Proceedings for the Geothermal Resources Council 38th Annual Meeting, Las Vegas NV, (2014).

Elliot, T.R., Buscheck, T.A., and Celia, M.A.: Active CO2 reservoir management for sustainable geothermal energy extraction and reduced leakage, Greenhouse Gases: Science and Technology, 1, (2013), 1-16.

Fenghour, A., Wakeham, W.A., and Vesovic, V.: The viscosity of carbon dioxide. J. Phys. Chem. Ref. Data, 27 (1), (1998), 31–44.

Garapati N., Randolph, J.B., and Saar M.O.: Brine displacement by CO2, heat energy extraction rates, and lifespan of an axis-symmetric CO2 Plume Geothermal system with a vertical injection and a horizontal production well, to be submitted to Geothermics, (2014).

Hao, Y., Sun, Y., and Nitao, J.J.: Overview of NUFT: A versatile numerical model for simulating flow and reactive transport in porous media, Chapter 9 in Groundwater Reactive Transport Models, (2012), 213-240.

Lemmon, E.W. and Jacobsen, R.T.: Viscosity and thermal conductivity equations for nitrogren, oxygen, argon, and air, International Journal of Geophysics, 25 (1), (2004), 21-69.

Nitao, J.J.: "Reference manual for the NUFT flow and transport code, version 3.0," Lawrence Livermore National Laboratory, UCRL-MA-130651-REV-1, Livermore, CA (1998).

OASIS: California ISO Open Access Same-time Information System (OASIS), http://oasis.caiso.com/mrioasis/logon.do, accessed February, (2014).

Pruess, K.: Enhanced geothermal systems (EGS) using CO2 as working fluid–a novel approach for generating renewable energy with simultaneous sequestration of carbon, Geothermics, 35, (2006), 351-367.

Randolph, J.B. and Saar, M.O.: Coupling carbon dioxide sequestration with geothermal energy capture in naturally permeable, porous geologic formations: Implications for CO2 sequestration. Energy Procedia, 4, (2011a), 2206-2213.

Randolph, J.B. and Saar, M.O.: Impact of reservoir permeability on the choice of subsurface geothermal heat exchange fluid: CO2 versus water and native brine. Proceedings for the Geothermal Resources Council 35th Annual Meeting, San Diego, CA, (2011b).

Randolph, J.B., and Saar, M.O.: Combining geothermal energy capture with geologic carbon dioxide sequestration, Geophysical Research Letters, 38, (2011c).

Saar, M.O., Randolph, J.B., and Kuehn, T.H.: Carbon Dioxide-based geothermal energy generation systems and methods related thereto. US Patent Application 20120001429, international patents pending, (2010).

Saar, M.O., Buscheck, T.A., Jenny, P., Garapati, N., Randolph, J.B., Karvounis, D.C., Chen, M., Sun, Y., and Bielicki, J.M.: Numerical study of multi-fluid and multi-level geothermal system performance, Proceedings for the World Geothermal Congress 2015, Melbourne, Australia, in review, (2015).

Span, R. and Wagner, W.: A new equation of state for carbon dioxide covering the fluid region from the triple-point temperature to 1100K at pressures up to 800 MPa. Journal of Physical and Chemical Reference Data, 25, (1996), 1509-1596.

Span, R., Lemmon, E.W., Jacobsen, R.T., Wagner, W., and A. Yokozeki, A.: A reference equation of state for the thermodynamic properties of nitrogen for temperatures from 63.151 to 1000 K and pressures to 2200 MPa, Journal of Physical and Chemical Reference Data, 29 (6), (2000), 136-1433.

van Genuchten, M.T.: A closed form equation for predicting the hydraulic conductivity of unsaturated soils. Soil Science Society of America Journal, 44, (1980), 892-898.

Zhou, Q., Birkholzer, J.T., Tsang C-F., and Rutqvist, J.A.: A method for quick assessment of CO2 storage capacity in closed and semi-closed saline formations. International Journal of Greenhouse Gas Control, 2, (2008), 626-639.